Fabrication of magnetic bio-Au nanoclusters by using SlaA-layer ghosts of *Sulfolobus acidocaldarius* as a template

S. Selenska-Pobell [*], T. Reitz [*], A. Geissler [*], T. Herrmannsdörfer [**] and M.L. Merroun [***]

[*] Institute of Radiochemistry, HZDR, Dresden, Germany, s.selenska-pobell@hzdr.de
[**] Dresden High Magnetic Field Laboratory, HZDR, Dresden, Germany, t.herrmannsdoerfer@hzdr.de
[***] Department of Microbiology, University of Granada, Granada, Spain, merroun@ugr.es

ABSTRACT

Gold nanoparticles with a size of about 2.5 nm were produced using the SlaA-layer ghosts of the archaeon *Sulfolobus acidocaldarius* as a template. These archaeal bio-Au nanoparticles differ significantly from those of the bacterial bio-Au nanoparticles produced earlier on the S-layer of *Bacillus sphaericus*. The archaeal Au nanoparticles consist exclusively of Au(0), while the bacterial ones represent a mixture of Au(0) and Au(III). The most impressive feature of the archaeal Au nanoparticles is that they are paramagnetic, in contrast to the bacterial ones and also to bulk gold which are diamagnetic. As demonstrated by SQUID magnetometry, the archaeal bio-Au possesses an unusually large magnetic moment of about 0.1 μ_B/Au atom. HR-TEM combined with EDX analysis revealed that the archaeal Au nanoparticles are linked to sulfur atoms. The latter originate from the thiol groups of the cystein amino acid residues which are characteristic for the SlaA-layer of *S. acidocaldarius* but absent in the S-layer of *B. sphaericus*.

Keywords: Magnetic gold nanoparticles, *Sulfolobus acidocaldarius*, surface layer (S-layer)

1 INTRODUCTION

Production, characterization, and application of nano-sized particles of noble metals are fast developing topics of modern science and technology. The properties of nano-scaled particles are often unusual and depend on their size and shape mostly due to the dramatically increased number of surface atoms in comparison to their volume [1, 2]. Nano-sized noble metal particles can be used in catalysis [3, 4], biomedicine [5], as optical bio- and chemosensors [6, 7], and for environmental remediation [8]. Along with the large variety of abiotic templates used for the production of metallic nanoparticles, biological substrates are of increasing interest. The biological substrates are advantageous as they provide a non-toxic and therefore environmentally friendly matrix for fabrication of metallic nano-structures. In the present work empty cell ghosts consisting of the S-layer protein called SlaA [9] of the acidothermophilic crenarchaeon *Sulfolobus acido-caldarius* were used as a matrix for the synthesis of metallic Au nanoparticles. The produced archaeal Au nanoparticles differ from those produced earlier on the bacterial S-layer sheets of *Bacillus sphaericus* [10, 11] in their size and the grade of reduction of Au(III) to Au(0) during the production. In addition, the archaeal Au nanoparticles, in contrast to the bacterial ones, exhibit paramagnetic properties, which might be related to their size and the association with the thiol groups, specific for the SlaA protein only. Interestingly, the magnetism of the archaeal bio-Au is much stronger than those published for chemically synthesized [12] and even thiol capped [13] Au nanoparticles.

2 MATERIALS AND METHODS

2.1 Production of the Au-nanoparticles

The S-layer sheets of *B. sphaericus* and the SlaA-ghosts of *S. acidocaldarius* were purified as described earlier [10, 14]. The production of the Au nanoparticles was performed according to [12] in a two-step procedure by using DMAB as a reducing agent. Bearing in mind that the inside surface of the S-layers facing the cells is negatively charged [15], we assume that the initial deposition of Au(III) occurs inside of the SlaA ghosts. The thiol containing cystein amino acid residues of the SlaA protein of *S. acidocaldarius* are suggested to play an important role for the physico-chemical stability of the protein lattices of this thermoacidophilic archaeon [16] and they possess, in addition, a strong affinity to Au [13]. In our former work we have demonstrated, however, that the bacterial S-layer sheets of *B. sphaericus* JG-A12, which does not contain thiol groups, can also serve as efficient template for Au-nanoclusters formation [10, 11]. Although the underlying mechanisms for the Au(III) binding in both cases are not clear we expected, that in the case of the here studied archaeon the deposition and the reduction of Au (III) should be more efficient due to the thiol groups present in it.

2.2 Transmission Electron Microscopic (TEM) analyses combined with Energy Dispersive X-ray spectroscopy (EDX)

Before TEM analyses the metallized SlaA-ghosts were disrupted into SlaA-layer sheets by sonication using Branson W-250D Ultrasonifier. Both the archaeal and bacterial bio-Au nanoparticles were dehydrated with ethanol and deposited on a carbon coated copper TEM grid.

TEM analyses were performed in a high resolution Philips CM 200 transmission electron microscope at an acceleration voltage of 200 kV. EDX analysis, which provides information about the elemental surrounding of the Au, was performed at the same voltage using a spot size of 7 nm and a live counting time of 200 s.

2.3 X-ray Photoelectron Spectroscopy (XPS) measurements

The XPS measurements of the monolayer fragments of the sonified metallized SlaA-ghosts were performed using a scanning auger electron spectrometer (Microlab 310F, Fisions instruments) with field-emission cathode and hemispherical sector analyzer with accessory XPS-unit (Al/Mg - X-ray tube). The X-ray spot had a size of about 2 x 3 mm^2. Measurements were conducted in CAE mode using a pass energy of 10 eV. The carbon 1s peak (284.6 eV) was used for energy calibration.

2.4 SQUID measurements

Magnetization measurements were performed using a Superconducting Quantum Interference Device (SQUID) magnetometer. A small part of the prepared archaeal and bacterial bio-Au were fixed in a specially designed sample holder. During the measurements, the magnetic field was held constant ($B_0 = 2$ T) in the superconducting magnetic field coil while the samples were moved through a pick-up coil system of the flux transformer connected to the SQUID. Magnetization data were taken at temperatures $1.8\ K \leq T \leq 300$ K using a liquid-He cooled variable-temperature insert installed in the commercial SQUID-magnetometer set up (MPMS, Quantum Design, Inc., San Diego, USA). In order to scale the measured magnetic moments to the amount of substance, the weight of the sample was determined. For calculating the magnetic moment arising from each single gold atom, the proportion of gold in the sample was additionally calculated on the basis of ICP-mass spectroscopic data. Hypothetical iron impurities, which could skew magnetic results, were checked and excluded in all samples studied.

3 RESULTS AND DISCUSSION

3.1 Properties of the purified SlaA-layer ghosts

As evident from the results presented in Fig. 1, no intact cells were present in the purified fraction of the SlaA-layer ghosts. The latter (Fig. 1B) possess the shape and the size of the intact cells of *S. acidocaldarius* (Fig. 1A) but are translucent which indicates that they are free of cellular compounds.

The SDS-PAGE analysis of the denatured to monomers ghosts demonstrated only one protein band with an estimated molecular mass of about 150 kDa (not shown). This result is well in line with the molecular weight, calculated for the SlaA protein from it's primary structure [9].

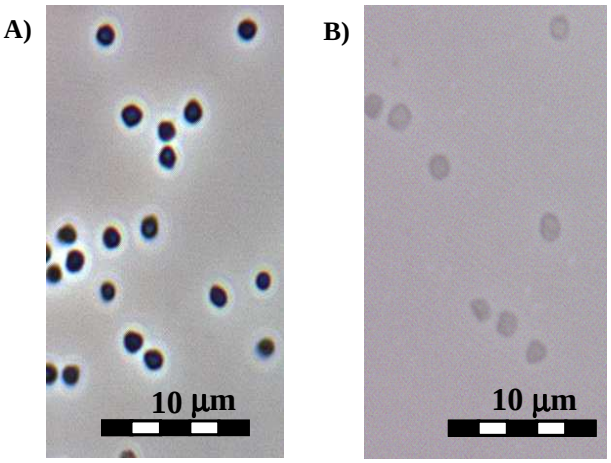

Figure 1. Light microscopic pictures of: A) intact cells of *S. acidocaldarius* and B) SlaA-ghosts.

3.2 Characterization of the Au nanoparticles

The formed gold nanoparticles were visualized by high resolution TEM coupled with EDX. As shown in Fig. 2, the Au nanoparticles were distributed rather irregularly on the bacterial as well as on the SlaA-layer lattices and did not reveal a regular pattern. The recorded EDX spectrum of a single SlaA-Au nanoparticle exhibits energy peaks which are specific for gold, as well as for carbon, oxygen, sulfur, and copper (Fig. 2A). The carbon and copper peaks arise from the carbon-coated copper grid supporting the TEM sample. The large sulfur peak close to the Au peak suggests that the gold nanoparticles are associated with the sulfur of the thiol groups of the SlaA protein (Fig. 2A). The average size of these particles was about 2.5 nm. The bacterial gold nanoparticles observed by TEM on the S-layer of *B. sphaericus* JG-A12 (Fig. 2B) are bigger with an average size of about 4 nm and their number per unit of area is substantially larger compared to the archaeal bio-Au. As expected, no sulfur was associated with the bacterial bio-Au, due to the absence of thiol groups in the bacterial S-layer (Fig. 2B, here the additional peack corresponds to Si). Another difference between the two kinds of gold nanoclusters is that in the case of the archaeal bio-Au all nanoclusters are electron dense, dark spots, while those of the bacterial bio-Au represent a mixture of dark and less dark, semi-translucent nanoclusters. These low dense spots in the case of bacterial bio-Au may possibly represent gold accumulates consisting mainly of unreduced Au(III). This suggestion is in agreement with our results published earlier, that in the gold nanoparticles formed on the S-layer sheets of *B. sphaericus* JG-A12 only an average of about

40% of the Au(III) was reduced to Au(0) [10]. The presence of the bigger, electron dense black spots in the case of the bacterial bio-Au shown in Fig. 2B could also be explained by additional reduction of Au(III) to Au(0) by the electron beam during the TEM measurements and possibly aggregation of some of the formed nanoclusters.

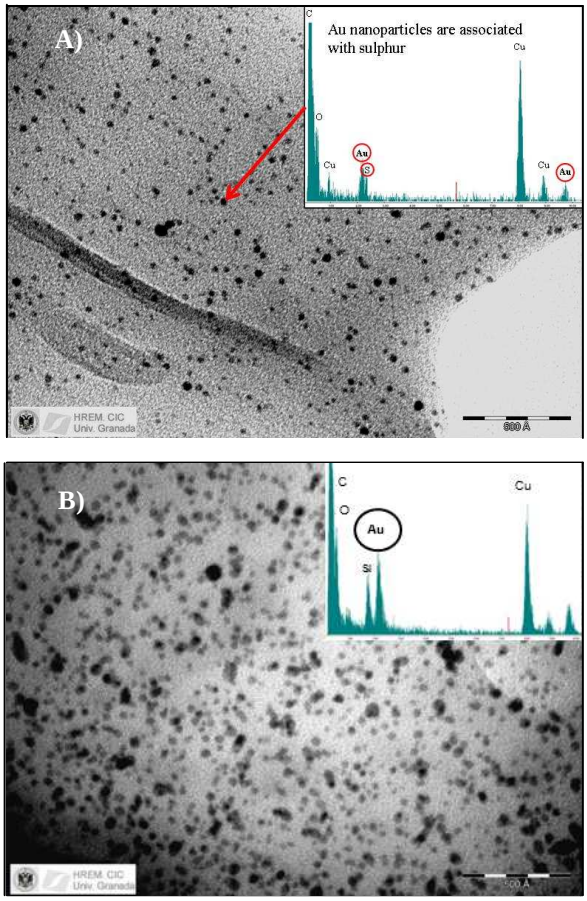

Figure 2. Transmission electron micrographs of gold nanoparticles and EDX spectra: A) SlaA-layer of *S. acidocaldarius;* B) S-layer of *B. sphaericus*

No such translucent particles were found in the TEM pictures of the archaeal bio-gold (Fig. 1A) indicating that all Au-nanoparticles in this case are metallic. In order to determinate the amount of reduced metallic Au(0) in the archaeal bio-Au samples we used X-ray Photoelectron Spectroscopy (XPS). The XPS spectrum possess the typical gold 4f double peak, Au 4f (7/2) and Au4f(5/2), at positions characteristic for metallic gold while no peak for Au(III) was found (not shown). This analysis clearly demonstrates that most of the gold present in the archael samples is in its metallic state. The zero-valent oxidation state of gold additionally supports the assumption that the gold-thiol bond does not have the characteristics of gold sulphide and suggests another complexation mode. The almost complete reduction of Au(III) to Au(0) in the case of the archaeal SlaA-ghosts as a template for the nanoclusters fabrication is in contrast to the partial Au(III) reduction occurring on the bacterial S-layer templates. This difference is possibly connected to the rather different way of deposition and reduction of Au(III) in the archaeal ghosts and on the bacterial S-layer sheets. In contrast to the bacterial S-layers, where Au(III) is deposited on free swimming sheets, in the case of the SlaA-ghosts the initial deposition of Au(III) cations is occuring inside of them onto the negatively charged inner side of the SlaA-layer, which in the intact cells is turned to the cell [15]. Hence, the gold solution has to be infiltrated into the ghosts through the SlaA-lattice. During this infiltration the Au(III) cations will be caught by the metal-binding ligands of the inner face of the SlaA-layer and deposited there in a way, which we have already described for the deposition of Pd in the whole cells of *B. sphaericus* [3]. The thiol groups of the SlaA-ghosts should contribute to the effective binding and even to partial initial reduction of Au(III). Hence, in the case of the archaeal ghosts, not the whole gold solution but only that part of it which is infiltrated into them is involved in the gold deposition in which thiol groups may play a dominant role. Our results demonstrate that the archaeal nanoclusters are smaller, consisting mostly of Au(0), and are also differently organized than those produced on the bacterial S-layer sheets.

3.2. Magnetic properties of the Au nanoparticles

SQUID magnetometry demonstrated that the archaeal Au(0) nanoparticles are paramagnetic and possess a magnetic moment of about 0.1 μ_B per gold atom. This moment is substantially larger than the ones observed for thiol-capped Au nanoclusters [13] and other chemically produced nanoparticles [12]. Interestingly, no magnetic properties were observed for the somewhat larger (about 4 nm instead of 2.5 nm) bacterial Au-nanoparticles formed on the above mentioned thiol-free bacterial S-layer of *B. sphaericus*. Possible reasons for that may be the fact that they are not fully reduced to Au(0), that they are bigger, and that they are not bound to thiol groups. Therefore, we suggest that the magnetic properties of the archaeal gold nanoparticles formed by using the SlaA-ghosts as a template are connected to their full reduction to Au(0), and most likely also depend on both, the transfer of electrons from Au to S to form the binding of Au to the thiol groups, and possibly the size of the formed nanoparticles. These size and ligand effects determine the number of holes in the *d*-electron band of gold, which in turn influences the magnetic behavior of the formed gold nanoparticles [2, 12].

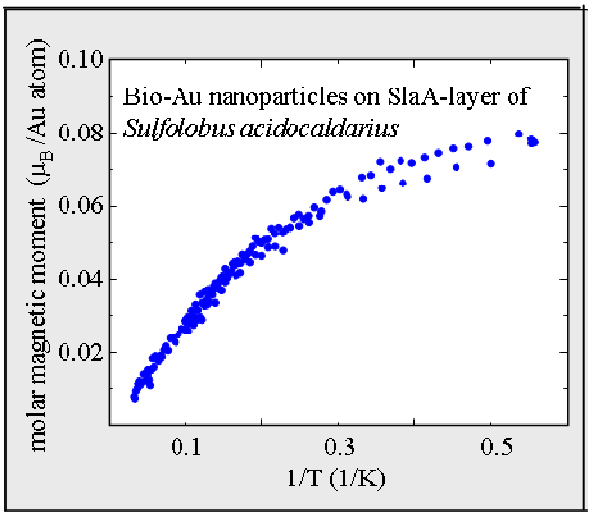

Figure 3. Temperature dependence of the magnetic moments of the Au nanoparticles formed on the SlaA-layer ghosts of *S. acidocaldarius*, scaled to one gold atom.

4 CONCLUSIONS

In this study we have demonstrated that the SlaA ghosts of *S. acidocaldarius* serve as a more effective template for complete reduction of Au(III) to Au(0) than the S-layer of *B. sphaericus*. Moreover, in contrast to *B. sphaericus* S-layer sheets, SlaA ghosts are an excellent template for formation of magnetic bio-Au(0). The advantages of the SlaA-ghost matrix are related to its unusual shape and biochemical characteristics both responsible for precise deposition of gold cations. The thiol groups of the SlaA protein are most likely essential for the initial deposition of Au(III) inside the SlaA ghosts, its efficient reduction, and the evocation of magnetism in reduced Au(0) nanoparticles.

Acknowledgement: We thank Frank Pobell for the fruitful discussions and critical reading of the manuscript. The contribution of M. Merroun was supported by "Ministerio de Ciencia e Innovación", Spain (grant No. CGL2009-09760).

REFERENCES

[1] L. He, Unexpected magnetic moments in ultrafine diamagnetic systems. J. Phys. Chem. C, 114, 12487-12489, 2010.

[2] P. Zhang, T.K. Sham, X-ray studies of the structure and electronic behavior of alkanethiolate-capped gold nanoparticles: The interplay of size and surface effects. Phys. Rev. Lett. 90, 245502-1 – 245502-4, 2003.

[3] N. Creamer, I. Mikheenko, P. Yong, K. Deplanche, D. Sanyahumbi, J. Wood, K, Pollmann, M. Merroun, S. Selenska-Pobell, L.E. Macaskie, Novel supported Pd hydrogenation bionanocatalyst for hybrid homogeneous/heterogeneous catalysis. Catalysis Today 128, 80-87, 2007.

[4] M.Haruta, When gold is not noble: Catalysis by nanoparticles. The Chemical Record 3, 75-87, 2003.

[5] W. Cai, T. Gao, H. Hong, , J. Sun, Applications of gold nanoparticles in cancer nanotechnology. Nanotechnology Sci & Appl. 1, 17-32, 2008.

[6] A.J. Haes, S.L, Zou, G.C.V. Schatz, R.P.Duyne, A nanoscale optical biosensor: The long range distance dependence of the localized surface plasmon resonance of noble metal nanoparticles. J Phys. Chem. B 108, 6961-6968, 2004.

[7] M.H. Kim, S. Kim, H.H. Jang, S. Yi, S.H. Seo, M.S. Han, A gold nanoparticle-based colorimetric sensing ensemble for the colorimetric detection of cyanide ions in aqueous solution. Tetrahedron Lett. 51, 4712-4716, 2010

[8] T.A. Pradeep, Noble metal nanoparticles for water purification: A critical review. Thin Solid Films 517, 6441-6478, 2009.

[9] A. Veith, A. Klingl, B. Zolghadr, K. Lauber, R. Mentele, F. Lottspeich, R. Rachel, S.V. Albers, A. Kletzin *Acidianus, Sulfolobus* and *Metallosphaera* surface layers: Structure, composition and gene expression. Mol. Microbiol. 73, 58-72, 2009.

[10] M. Merroun, A. Rossberg, C. Hennig, A. Scheinost, S. Selenska-Pobell, Spectroscopic characterization of gold nanoparticles formed by cells and S-layer protein of *Bacillus sphaericus* JG-A12. Mat. Sci. Eng. C-Bio S 27,188-192, 2007.

[11] U. Jankovski, M. Merroun, S. Selenska-Pobell, K. Fahmy S-layer protein of *Lysinibacillus sphaericus* JG-A12 as matrix for Au(III) sorption and nanoparticles formation. Spectroscopy 24, 1-2, 177-181, 2010.

[12] Y. Yamamoto, T. Miura, M. Suzuki, N, Kawamura, H. Miyagawa, T. Nakamura, K. Kobayashi, T. Teranishi, H. Hori, Direct observation of ferromagnetic spin polarization in gold nanoparticles. Phys. Rev. Lett. 93, 116801-1 – 116801-4, 2004.

[13] P. Crespo, R. Litran, T.C. Rojas, M. Multigner, J.M. de la Fuente, J.C. Sanchez-Lopez, M.A. Garcia, A. Hernando, S. Penades, A. Fernandez, Permanent magnetism, magnetic anisotropy, and hysteresis of thiol-capped gold nanoparticles. Phys. Rev. Lett. 93, 087204-1 – 087204-4, 2004.

[14] D. Grogan, Isolation and fractionation of cell envelope from the extreme thermo-acidophile *Sulfolobus Acidocaldarius*. J. Microbiol. Methods, 26, 35-43, 1996.

[15] D. Pum, M. Sara, U.B. Sleytr, Structure, surface charge, and self-assembly of the S-layer lattice from *Bacillus coagulans* E38-66. J. Bacteriol. 171, 5296-5303, 1989.

[16] H. Engelhardt, Are S-layers exoskeletons? The basic function of protein surface layers revisited. J. Struct. Biol. 160, 115-124, 2007.